Electronic Supplementary Material (ESI) for ChemComm.

Supplementary Information

Hydrogenation of an Iridium-Coordinated Imidazol-2-ylidene Ligand Fragment

Martín Hernández-Juárez,[a] Joaquín López-Serrano,*[,a] Pablo González-Herrero,[b] Nuria Rendón,[a] Eleuterio Álvarez,[a] Margarita Paneque,*[,a] and Andrés Suárez*[,a]

[a] *Instituto de Investigaciones Químicas (IIQ), Departamento de Química Inorgánica and Centro de Innovación en Química Avanzada (ORFEO-CINQA), CSIC and Universidad de Sevilla.*

[b] *Departamento de Química Inorgánica. Facultad de Química, Universidad de Murcia.*

E-mail: joaquin.lopez@iiq.csic.es; paneque@iiq.csic.es; andres.suarez@iiq.csic.es

Table of Contents

1. Synthetic procedures and analytical data

1.1. General procedures

All reactions and manipulations were performed under nitrogen or argon, either in a Braun Labmaster 100 glovebox or using standard Schlenk-type techniques. All solvents were distilled under nitrogen with the following desiccants: sodium-benzophenone-ketyl for diethyl ether (Et_2O) and tetrahydrofuran (THF); sodium for pentane and toluene; CaH_2 for dichloromethane and acetonitrile (CH_2Cl_2, CH_3CN); and NaOMe for methanol (MeOH). Iridium complex **1** was prepared as previously described.[1] All other reagents were purchased from commercial suppliers and used as received. NMR spectra were obtained on Bruker DPX-300, DRX-400, AVANCEIII/ASCEND 400R or DRX-500 spectrometers. $^{31}P\{^1H\}$ NMR shifts were referenced to external 85% H_3PO_4, while $^{13}C\{^1H\}$ and ^1H shifts were referenced to the residual signals of deuterated solvents. All data are reported in ppm downfield from Me_4Si. All NMR measurements were carried out at 25 °C, unless otherwise stated. NMR signal assignations were confirmed by 2D NMR spectroscopy (^1H-^1H COSY, ^1H-^1H NOESY, ^1H-^{13}C HSQC and ^1H-^{13}C HMBC) for all the complexes. Elemental analyses were run by the Analytical Service of the Instituto de Investigaciones Químicas in a Leco TrueSpec CHN elemental analyzer. IR spectra were acquired on a Bruker Tensor 27 instrument.

UV-vis absorption spectra were recorded on a Perkin-Elmer Lambda 750S spectrophotometer. Excitation and emission spectra were recorded on a Jobin Yvon Fluorolog 3-22 spectrofluorometer with a 450 W xenon lamp, double-grating monochromators, and a TBX-04 photomultiplier. The solid-state measurements were made in a front-face configuration using polycrystalline samples between quartz coverslips; the solution measurements were carried out in a right angle configuration using degassed solutions of the samples in 5 mm quartz NMR tubes. Emission lifetimes (τ) were measured using either the Fluorolog's FL-1040 phosphorimeter accessory (τ > 10 μs) or an IBH FluoroHub TCSPC controller and a NanoLED pulse diode excitation source (τ < 10 μs); the estimated uncertainty is ±10% or better. Emission quantum yields (Φ) were measured using a Hamamatsu C11347 Absolute PL Quantum Yield Spectrometer; the estimated uncertainty is ±5% or better.

1.2. Synthesis and characterization of complexes 2 and 2(BF_4)

Complex 2. A suspension of **1** (0.354 g, 0.44 mmol) in toluene (15 mL) was heated to 120 °C for 12 h. The solvent of the resulting suspension was filtered off, and the solid was washed with cold THF (3 × 3 mL) and Et_2O (3 × 3 mL) and dried under vacuum. Complex **2** was isolated as a yellow solid (0.256 g, 84%). Low solubility of the complex in common deuterated solvents (CD_2Cl_2, THF-d_8, toluene-d_8, CD_3CN, DMSO-d_6) has precluded its full spectroscopic characterization. Crystals suitable for X-ray diffraction analysis were grown from a saturated solution of complex **2** in THF.

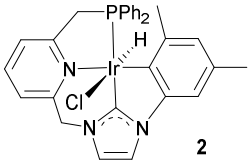

2

UV-vis (CH_2Cl_2): λ (ε/M^{-1} cm^{-1}): 289 (sh, 5300), 336 (sh, 2200), 393 (2500) nm. Luminiscence (solid, 298 K): λ_{exc} = 366, 448 nm; λ_{em} = 506 nm, Φ = 0.281, τ = 2.1 (13%), 6.3 (87%) μs.

Elemental analysis calcd (%) for $C_{30}H_{28}ClIrN_3P$: C 52.28, H 4.10, N 6.10; found: C 52.27, H 4.15, N 6.08.

^{1}H NMR (300 MHz, CD_2Cl_2): δ 7.83 (m, 4H, 4 H arom PPh_2), 7.74 (dd, $^3J_{HH}$ = 7.7 Hz, $^3J_{HH}$ = 7.6 Hz, 1H, H arom Py), 7.56 (d, $^3J_{HH}$ = 7.7 Hz, 1H, H arom Py), 7.48 (s, 1H, H arom NHC), 7.41 (m, 6H, 6 H arom PPh_2), 7.30 (d, $^3J_{HH}$ = 7.6 Hz, 1H, H arom Py), 7.18 (s, 1H, H arom NHC), 6.86 (s, 1H, H arom Xyl), 6.61 (s, 1H, H arom Xyl), 5.92 (d, $^2J_{HH}$ = 15.8 Hz, 1H, NC*H*H), 5.40 (d, $^2J_{HH}$ = 15.8 Hz, 1H, NC*H*H), 4.41 (dd, $^2J_{HH}$ = 16.9 Hz, $^2J_{HP}$ = 9.6 Hz, 1H, PC*H*H), 4.05 (dd, $^2J_{HH}$ = 16.9 Hz, $^2J_{HP}$ = 10.7 Hz, 1H, PC*H*H), 2.32 (s, 3H, CH_3), 2.03 (s, 3H, CH_3), –22.76 (d, $^2J_{HP}$ = 17.4 Hz, 1H, IrH).

^{31}P{^{1}H} NMR (121 MHz, CD_2Cl_2): δ 8.9.

IR (Nujol): ν = 2201 cm^{-1} (IrH).

Complex 2(BF_4). A suspension of **2** (0.085 g, 0.12 mmol) and $NaBF_4$ (0.068 g, 0.62 mmol) in a 1:1 mixture of CH_2Cl_2 and MeCN (6 mL) was stirred for 48 h. The resulting suspension was filtered off, and the solvent was evaporated. The obtained solid was washed with Et_2O (2 × 3 mL) and pentane (3 × 3 mL), and dried under vacuum. Complex **2(BF_4)** was isolated as a light brown solid (0.075 g, 78%).

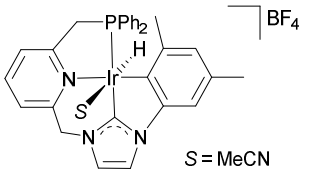

2(BF$_4$)

Elemental analysis calcd (%) for $C_{32}H_{31}BF_4IrN_4P\cdot CH_2Cl_2$: C 45.74, H 3.84, N 6.47; found: C 46.19, H 3.76, N 6.02.

^{1}H NMR (400 MHz, CD_2Cl_2): δ 7.93 (dd, $^3J_{HH}$ = 7.6 Hz, $^3J_{HH}$ = 7.6 Hz, 1H, H arom Py), 7.80 (dd, $^3J_{HP}$ = 11.1 Hz, $^3J_{HH}$ = 8.1 Hz, 2H, 2 H arom PPh_2), 7.72 (d, $^3J_{HH}$ = 7.7 Hz, 1H, H arom Py), 7.71 (d, $^3J_{HH}$ = 7.6 Hz, 1H, H arom Py), 7.59-7.49 (m, 10H, 8 H arom PPh_2 + 2 H arom NHC), 6.91 (s, 1H, H arom Xyl), 6.71 (s, 1H, H arom Xyl), 5.87 (d, $^2J_{HH}$ = 16.4 Hz, 1H, NC*H*H), 5.72 (d, $^2J_{HH}$ = 16.4 Hz, 1H, NC*H*H), 5.34 (s, CH_2Cl_2), 4.45 (dd, $^2J_{HH}$ = 17.6 Hz, $^2J_{HP}$ = 10.4 Hz, 1H, PC*H*H), 3.53 (dd, $^2J_{HH}$ = 17.6 Hz, $^2J_{HP}$ = 9.6 Hz, 1H, PC*H*H), 2.34 (s, 3H, CH_3), 2.14 (s, 3H, CH_3), 1.68 (s, 3H, CH_3CN), –20.62 (d, $^2J_{HP}$ = 18.0 Hz, 1H, IrH).

^{31}P{^{1}H} NMR (162 MHz, CD_2Cl_2): δ 17.0.

^{13}C{^{1}H} NMR (101 MHz, CD_2Cl_2): δ 172.3 (d, J_{CP} = 108 Hz, C^2 NHC), 166.4 (d, J_{CP} = 4 Hz, C_q arom), 155.8 (C_q arom), 148.9 (d, J_{CP} = 3 Hz, Ir-C_q arom), 146.4 (C_q arom), 138.8 (CH arom), 134.8 (d, J_{CP} = 13 Hz, 2 CH arom), 133.5 (C_q arom), 133.4 (C_q arom), 132.2 (CH arom), 132.0 (d, J_{CP} = 9 Hz, 2 CH arom), 131.6 (C_q arom), 130.7 (CH arom), 129.4 (d, J_{CP} = 11 Hz, 2 CH arom), 129.2 (d, J_{CP} = 9 Hz, 2 CH arom), 126.1 (CH arom), 125.8 (CH arom), 122.9 (d, J_{CP} = 9 Hz, CH arom), 121.4 (C_q arom), 120.2 (d, J_{CP} = 4 Hz, CH arom), 119.6 (N*C*CH$_3$), 116.0 (d, J_{CP} = 3 Hz, CH arom), 110.3 (CH arom), 56.7 (CH_2N), 50.5 (d, J_{CP} = 32 Hz, CH_2P), 29.3 (d, J_{CP} = 4 Hz, CH_3), 20.9 (CH_3), 3.0 (NC*C*H$_3$).

IR (Nujol): ν = 2169 cm^{-1} (IrH).

1.3. Synthesis and characterization of complex 3

To a suspension of complex **2** (0.250 g, 0.34 mmol) in THF (10 mL) was added a solution of KO^{t}Bu (0.042 g, 0.37 mmol) in THF (5 mL), and the reaction mixture was stirred for 24 h at room temperature. Solvent was evaporated, and the resulting solid was washed successively with H_2O (3 × 5 mL), Et_2O (2 × 5 mL), toluene (2 × 5 mL) and cold THF (2 × 5 mL), and dried under vacuum. Pale yellow solid (0.134 g, 60%). Crystals suitable for X-ray diffraction analysis were grown from a saturated solution of complex **3** in THF.

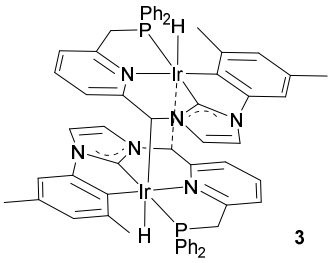

3

Elemental analysis calcd (%) for $C_{60}H_{54}Ir_2N_6P_2$: C 55.20, H 4.17, N 6.44; found: C 55.11, H 4.41, N 6.17.

^{1}H NMR (400 MHz, THF-d_8): δ 8.18 (dd, J_{HP} = 8.3 Hz, $^3J_{HH}$ = 7.8 Hz, 4H, 4 H arom PPh_2), 7.64 (m, 8H, 8 H arom PPh_2), 7.13 (m, 8H, 8 H arom PPh_2), 6.71 (s, 2H, 2 H arom), 6.57 (d, $^3J_{HH}$ = 6.8 Hz, 2H, 2 H arom Py), 6.52 (s, 2H, 2 H arom), 6.43 (s, 2H, 2 H arom), 6.39 (dd, $^3J_{HH}$ = 7.5 Hz, $^3J_{HH}$ = 7.5 Hz, 2H, 2 H arom Py), 5.81 (dd, $^3J_{HP}$ = 6.1 Hz, $^4J_{HH}$ = 3.1 Hz, 2H, 2 NCH-Py), 5.32 (d, $^3J_{HH}$ = 7.9 Hz, 2H, 2 H arom Py), 5.05 (s, 2H, 2 H arom), 4.21 (dd, $^2J_{HH}$ = 16.4 Hz, $^2J_{HP}$ = 10.0 Hz, 2H, 2 PC*H*H), 2.86 (dd, $^2J_{HH}$ = 16.1 Hz, $^2J_{HP}$ = 10.9 Hz, 2H, 2 PC*H*H), 2.50 (s, 6H, 2 CH_3), 2.22 (s, 6H, 2 CH_3), –15.80 (d, $^2J_{HP}$ = 22.0 Hz, 2H, 2 IrH).

^{31}P{^{1}H} NMR (162 MHz, THF-d_8, 318 K): δ 7.0.

IR (Nujol): ν = 1968 cm^{-1} (IrH)

1.4. Synthesis and characterization of complex 4

In a Fisher-Porter vessel, a suspension of **2** (0.250 g, 0.36 mmol) in THF (20 mL) cooled to 0 ^{o}C was pressurized with H_2 (2 bar) and treated with KO^{t}Bu (0.040 g, 0.36 mmol). The mixture was stirred for 48 h at room temperature, and the hydrogen pressure was carefully removed. Solvent was evaporated, and the residue was washed successively with H_2O (3 × 8 mL), toluene (3 × 8 mL), and cold THF (3 × 5 mL). Complex **4** was isolated after vacuum drying as a pale yellow solid (0.130 g, 57%). Crystals suitable for X-ray diffraction analysis were grown from a saturated solution of complex **4** in THF.

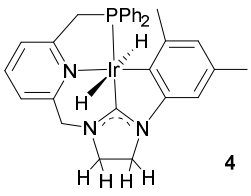

4

Elemental analysis calcd (%) for $C_{30}H_{31}IrN_3P$: C 54.86, H 4.76, N 6.40; found: C 54.89, H 4.76, N 6.33.

^{1}H NMR (400 MHz, THF-d_8): δ 8.09 (m, 4H, 4 H arom PPh_2), 7.52 (dd, $^3J_{HH}$ = 7.7 Hz, $^3J_{HH}$ = 7.7 Hz, 1H, H arom Py), 7.35 (m, 4H, 4 H arom), 7.24 (m, 3H, 3 H arom), 7.13 (d, $^3J_{HH}$ = 7.6 Hz, 1H, H arom Py), 6.24 (s, 2H, 2 H arom Xyl), 4.57 (s, 2H, NCH_2), 4.02 (m, 2H, CH_2 NHC), 3.95 (d, $^2J_{HP}$ = 9.7 Hz, 2H, PCH_2), 3.85 (m, 2H, CH_2 NHC), 2.21 (s, 3H, CH_3), 1.81 (s, 3H, CH_3), –9.43 (d, $^2J_{HP}$ = 21.6 Hz, 2H, IrH).

^{31}P{^{1}H} NMR (162 MHz, THF-d_8): δ 21.7.

^{13}C{^{1}H} NMR (101 MHz, THF-d_8): δ 213.4 (d, J_{CP} = 112 Hz, C^2 NHC), 165.9 (d, J_{CP} = 6 Hz, C_q arom), 157.9 (C_q arom), 150.1 (d, J_{CP} = 5 Hz, Ir-C_q arom), 144.5 (C_q arom), 138.2 (d, J_{CP} = 37 Hz, 2 C_q arom), 135.3 (CH arom), 135.3 (d, J_{CP} = 11 Hz, 4 CH arom), 130.2 (2 CH arom), 129.4 (C_q arom), 128.6 (d, J_{CP} = 10 Hz, 4 CH arom), 126.8 (C_q arom), 123.3 (CH arom), 122.0 (CH arom), 121.3 (d, J_{CP} = 8 Hz, CH arom), 107.2 (CH arom), 61.2 (CH_2N), 53.5 (d, J_{CP} = 4 Hz, CH_2 NHC), 53.0 (d, J_{CP} = 30 Hz, CH_2P), 46.8 (d, J_{CP} = 4 Hz, CH_2 NHC), 30.9 (d, J_{CP} = 6 Hz, CH_3), 21.3 (CH_3).

2. Monitoring by NMR spectroscopy of the reaction of 2 and H_2

In a J.Young-valved NMR tube, a suspension of **2** (0.010 g, 0.014 mmol) in THF-d_8 (0.5 mL) was pressurized with H_2 (1 bar) and treated with KO^{t}Bu (0.002 g, 0.014 mmol). The sample was analyzed by NMR spectroscopy after 40 min, observing the formation of the major complex **5**. Subsequent analysis of the sample after 2 days indicates the formation of complex **4**, along with minor amounts of **6** and **7**.

*Complex **5***

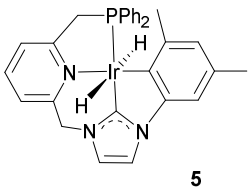

5

^{1}H NMR (400 MHz, THF-d_8): δ 8.10 (m, 4H, 4 H arom PPh_2), 7.54 (s, 1H, H arom NHC), 7.51 (dd, $^3J_{HH}$ = 7.6 Hz, $^3J_{HH}$ = 7.6 Hz, 1H, H arom Py), 7.32 (m, 6H, 6 H arom PPh_2), 7.15 (m, 3H, H arom NHC + 2 H arom Py), 6.76 (s, 1H, H arom Xyl), 6.33 (s, 1H, H arom Xyl), 5.29 (s, 2H, NCH_2), 3.96 (d, $^2J_{HP}$ = 9.9 Hz, 2H, CH_2P), 2.19 (s, 3H, CH_3), 1.79 (s, 3H, CH_3), –9.39 (d, $^2J_{HP}$ = 20.0 Hz, 2H, IrH).

$^{31}P\{^{1}H\}$ NMR (162 MHz, THF-d_8): δ 21.7.

$^{13}C\{^{1}H\}$ NMR (101 MHz, THF-d_8): δ 185.3 (d, J_{CP} = 116 Hz, C^2 NHC), 166.5 (d, J_{CP} = 6 Hz, C_q arom), 155.2 (C_q arom), 147.8 (d, J_{CP} = 4 Hz, C_q arom), 145.8 (C_q arom), 138.2 (d, J_{CP} = 38 Hz, 2 C_q arom), 135.1 (d, J_{CP} = 12 Hz, 4 CH arom), 134.9 (CH arom), 130.7 (d, J_{CP} = 4 Hz, IrC_q), 129.8 (d, J_{CP} = 1 Hz, 2 CH arom), 128.2 (d, J_{CP} = 9 Hz, 4 CH arom), 127.6 (C_q arom), 123.8 (CH arom), 123.5 (CH arom), 121.3 (d, J_{CP} = 9 Hz, CH arom), 117.9 (d, J_{CP} = 4 Hz, CH arom), 114.8 (d, J_{CP} = 3 Hz, CH arom), 108.5 (CH arom), 57.8 (CH_2N), 52.8 (d, J_{CP} = 30 Hz, CH_2P), 31.0 (d, J_{CP} = 6 Hz, CH_3), 20.8 (CH_3).

*Complex **6***

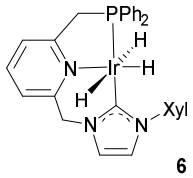

6

Complex **6** has been previously reported,[1] and detailed NMR data is only included for comparison purposes.

^{1}H NMR (400 MHz, THF-d_8): δ 7.78 (dd, $^{3}J_{HP}$ = 8.5 Hz, $^{3}J_{HH}$ = 8.5 Hz, 4H, 4 H arom PPh_2), 7.82 (s, 2H, 2 H arom), 7.50 (dd, $^{3}J_{HH}$ = 7.6 Hz, $^{3}J_{HH}$ = 7.6 Hz, 1H, H arom Py), 7.35 (m, 2H, 2 H arom), 7.24 (m, 6H, 6 H arom), 7.11 (m, 1H, H arom), 7.07 (s, 1H, H arom NHC), 6.94 (s, 1H, H arom NHC), 5.18 (s, 2H, CH_2N), 3.98 (d, $^{2}J_{HP}$ = 10.0 Hz, 2H, CH_2P), 2.38 (s, 6H, 2 CH_3), –9.98 (dd, $^{2}J_{HP}$ = 18.2 Hz, $^{2}J_{HH}$ = 4.8 Hz, 2H, IrH), –19.64 (dt, $^{2}J_{HP}$ = 14.4 Hz, $^{2}J_{HH}$ = 4.8 Hz, 1H, IrH).

$^{31}P\{^{1}H\}$ NMR (162 MHz, THF-d_8): δ 30.9.

$^{13}C\{^{1}H\}$ NMR (101 MHz, THF-d_8): δ 176.9 (d, J_{CP} = 121 Hz, C^2 NHC), 164.7 (d, J_{CP} = 6 Hz, C_q arom), 155.9 (C_q arom), 143.0 (C_q arom), 139.1 (d, J_{CP} = 42 Hz, 2 C_q arom), 137.2 (2 C_q arom), 134.3 (d, J_{CP} = 13 Hz, 4 CH arom), 134.1 (CH arom), 129.4 (2 CH arom), 128.2 (CH arom), 127.8 (d, J_{CP} = 10 Hz, 4 CH arom), 125.5 (2 CH arom), 121.3 (CH arom), 121.1 (d, J_{CP} = 9 Hz, CH arom), 120.5 (CH arom), 120.1 (d, J_{CP} = 4 Hz, CH arom), 59.9 (CH_2N), 49.2 (d, J_{CP} = 34 Hz, CH_2P), 21.2 (2 CH_3).

*Complex **7***

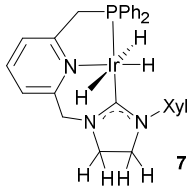

7

Complex **7** was not isolated due to the small amount of it found in the reaction mixtures. ^{1}H NMR spectroscopy signals of complex **7** could not be unambiguously assigned due to spectrum complexity, hence only the diagnostic signals for the hydride ligands are given.

^{1}H NMR (400 MHz, THF-d_8): δ –9.99 (dd, $^{2}J_{HP}$ = 18.3 Hz, $^{2}J_{HH}$ = 5.1 Hz, 2H, IrH), –19.94 (dt, $^{2}J_{HP}$ = 14.4 Hz, $^{2}J_{HH}$ = 5.1 Hz, 1H, IrH).

^{31}P{^{1}H} NMR (162 MHz, THF-d_8): δ 30.2.

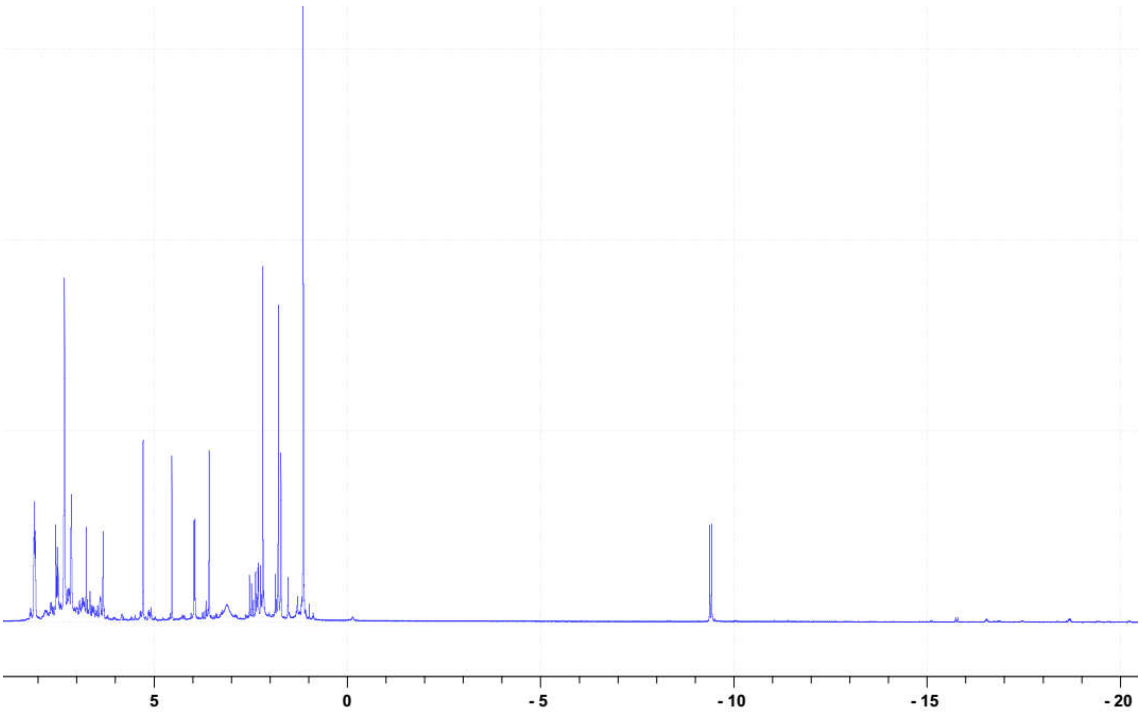

Figure S1. ^{1}H NMR spectrum of the reaction of **2** and H_2 in the presence of KO^{t}Bu after 40 min (400 MHz, THF-d_8).

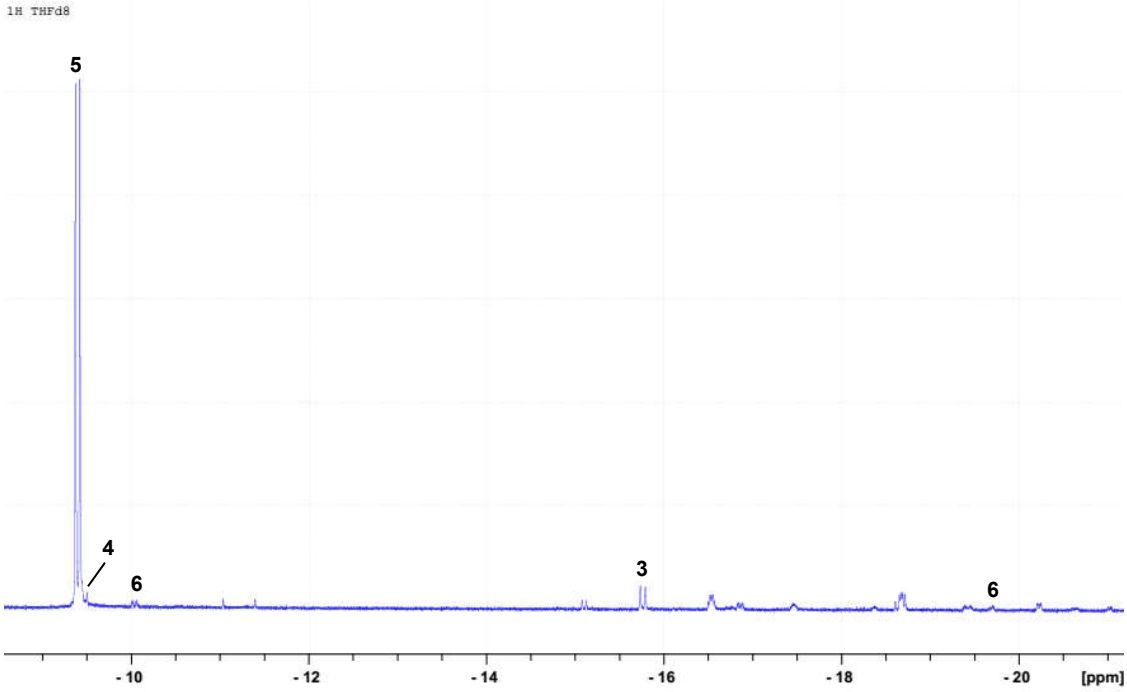

Figure S2. ^{1}H NMR spectrum (hydride region) of the reaction of **2** and H_2 in the presence of KO^{t}Bu after 40 min (400 MHz, THF-d_8).

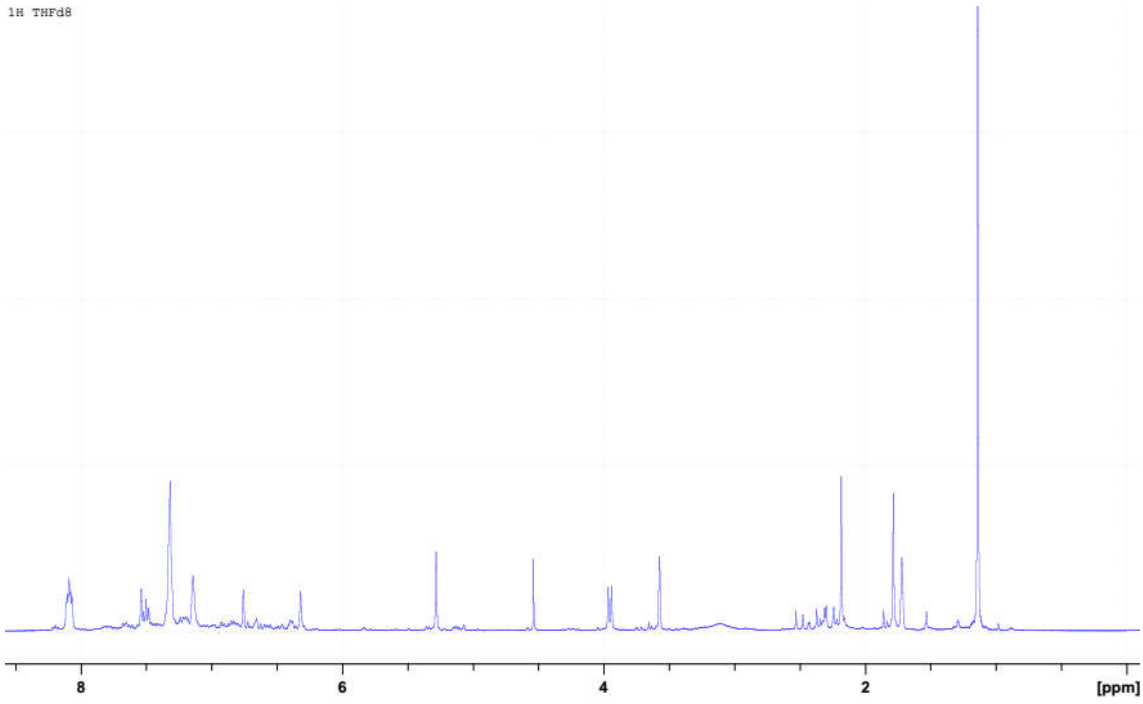

Figure S3. ^{1}H NMR spectrum (0-8.5 ppm region) of the reaction of **2** and H_2 in the presence of KO^{t}Bu after 40 min (400 MHz, THF-d_8).

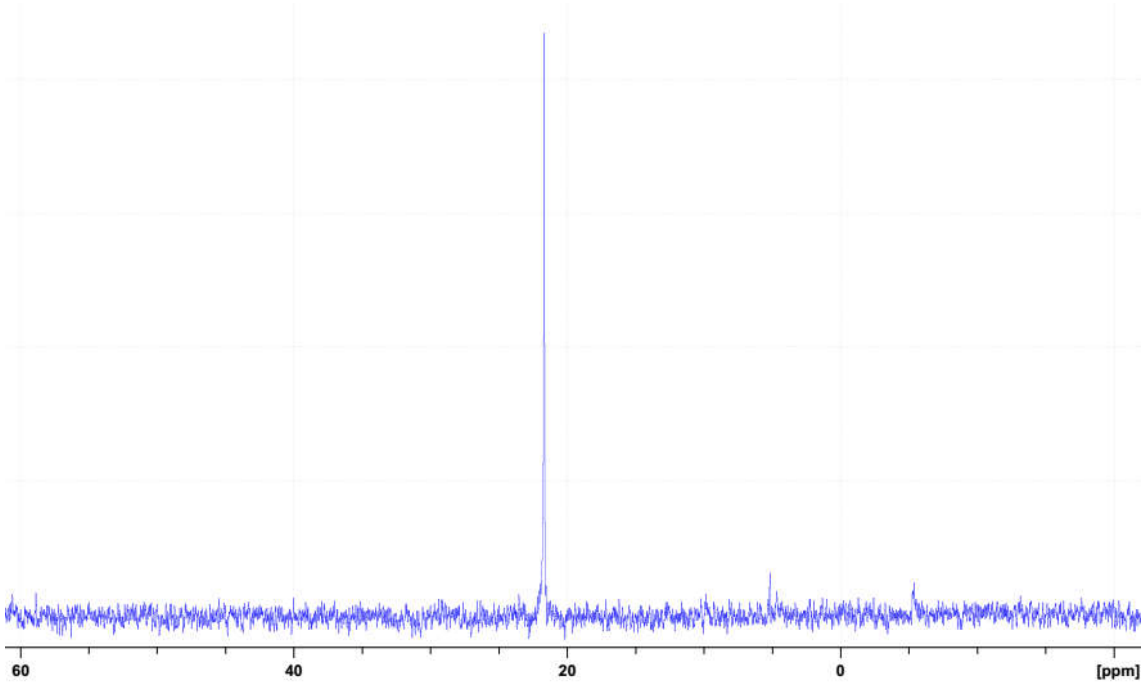

Figure S4. $^{31}P\{^{1}H\}$ NMR spectrum of the reaction of **2** and H_2 in the presence of KO^{t}Bu after 40 min (162 MHz, THF-d_8).

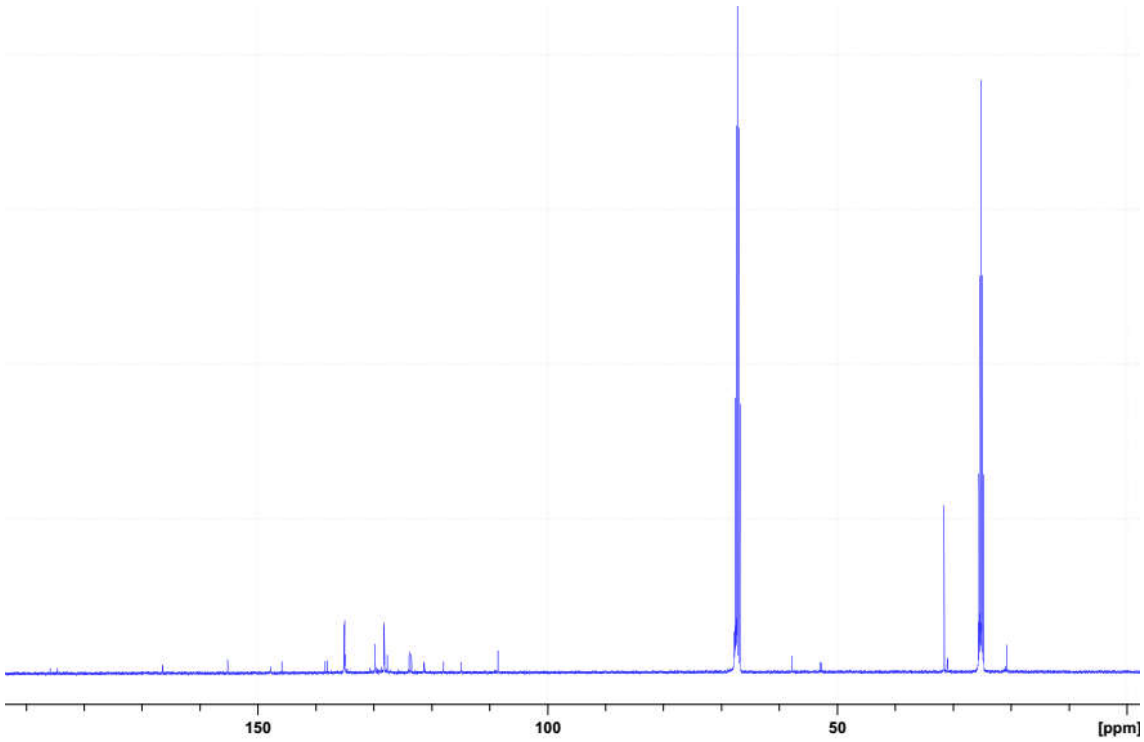

Figure S5. $^{13}C\{^{1}H\}$ NMR spectrum of the reaction of **2** and H_2 in the presence of KO^{t}Bu after 40 min (101 MHz, THF-d_8).

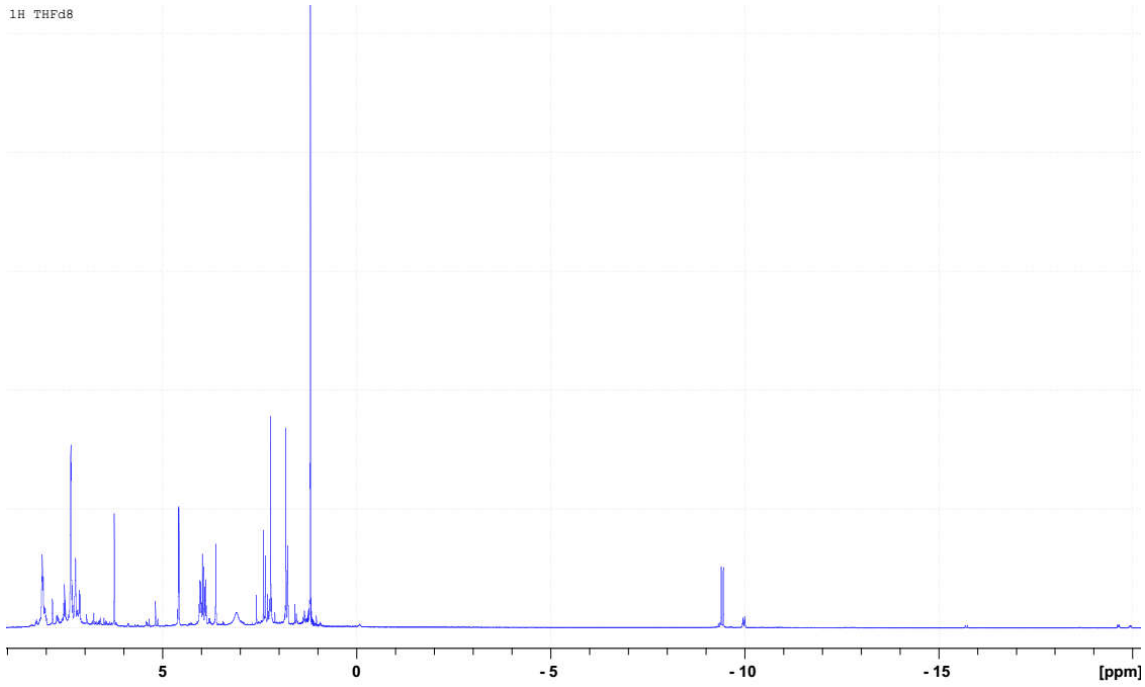

Figure S6. ^{1}H NMR spectrum of the reaction of **2** and H_2 in the presence of KO^{t}Bu after 48 h (400 MHz, THF-d_8).

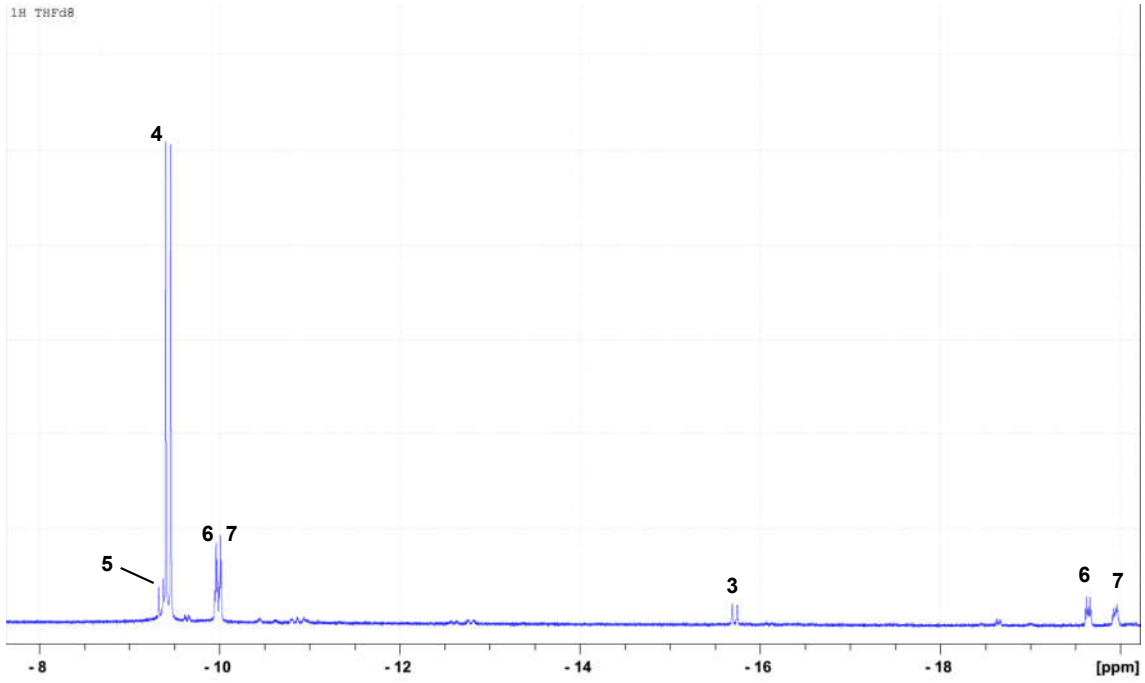

Figure S7. ^{1}H NMR spectrum (hydride region) of the reaction of **2** and H_2 in the presence of KO^{t}Bu after 48 h (400 MHz, THF-d_8).

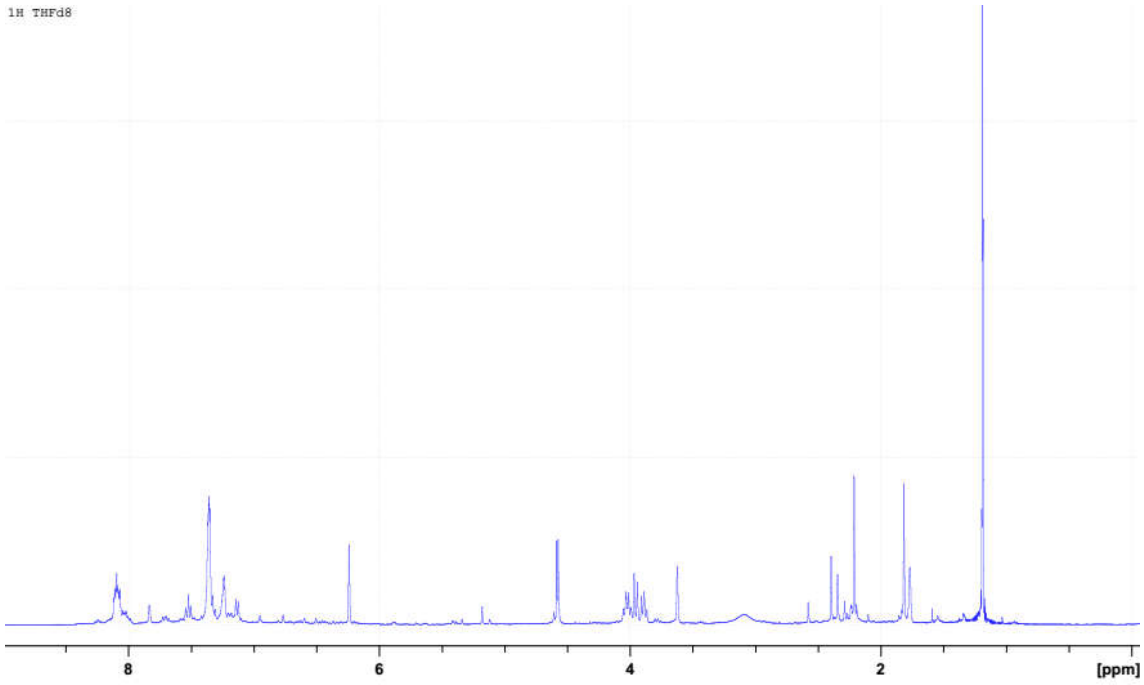

Figure S8. ^{1}H NMR spectrum (0-8.5 ppm region) of the reaction of **2** and H_2 in the presence of KO^{t}Bu after 48 h (400 MHz, THF-d_8).

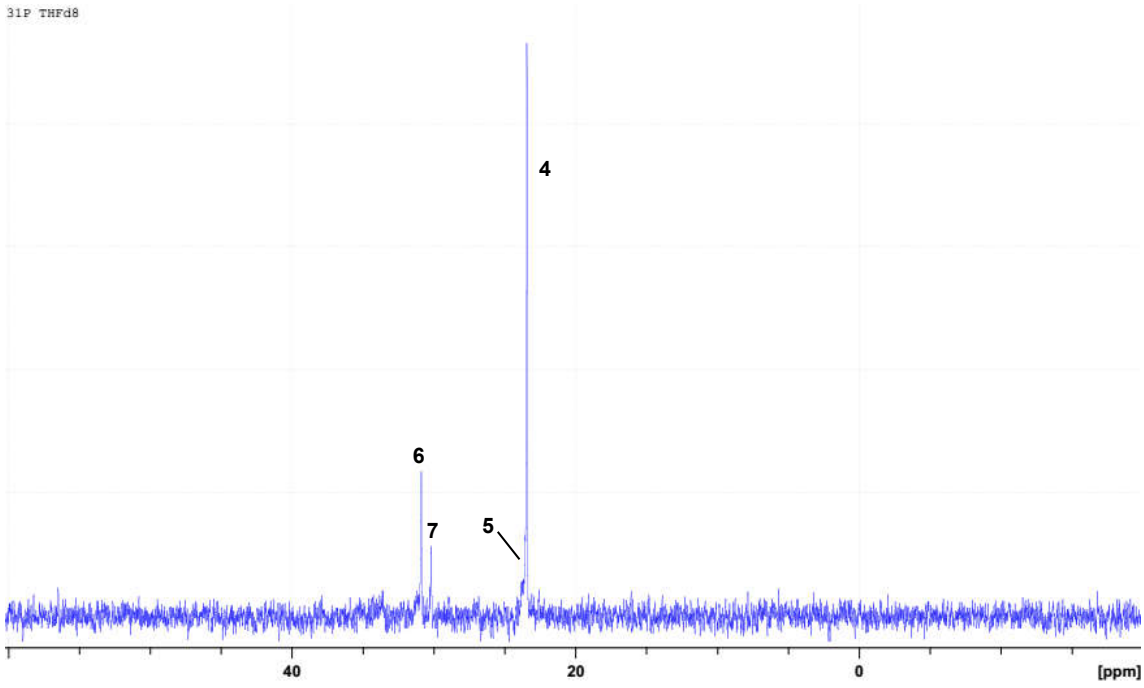

Figure S9. ^{31}P{^{1}H} NMR spectrum of the reaction of **2** and H_2 in the presence of KO^{t}Bu after 48 h (162 MHz, THF-d_8).

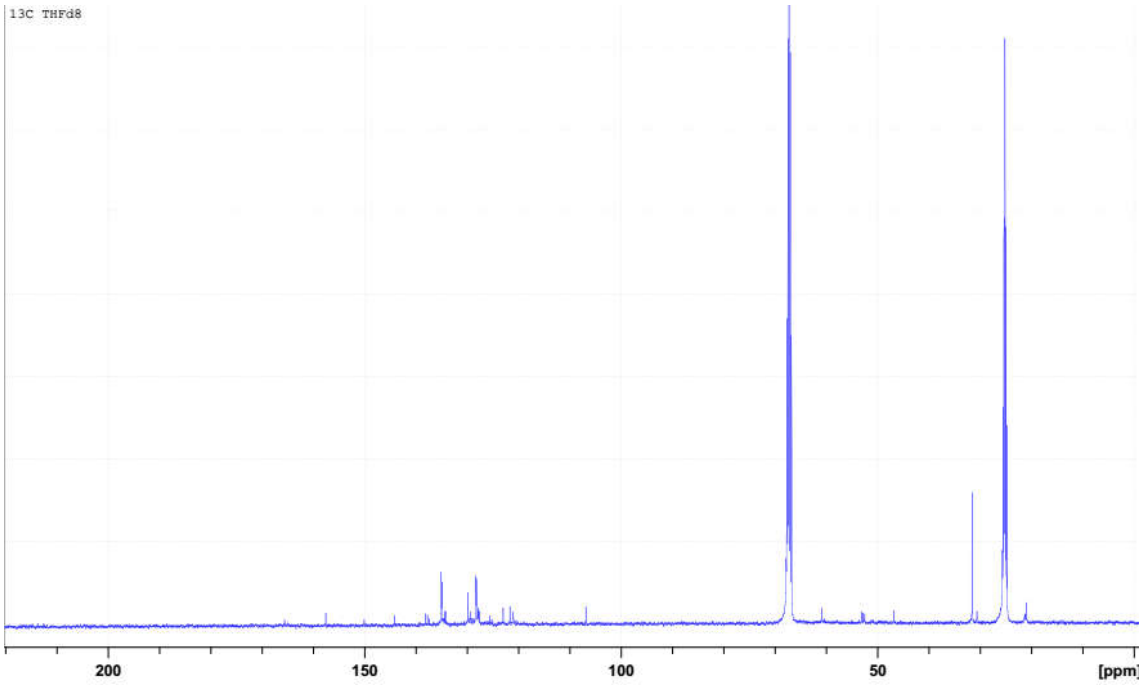

Figure S10. $^{13}C\{^{1}H\}$ NMR spectrum of the reaction of **2** and H_2 in the presence of KO^{t}Bu after 48 h (101 MHz, THF-d_8).

3. Control experiments involving complex 6

*Attempted reaction of **6** with H_2 to yield **7***

In a J.Young-valved NMR tube, a solution of **1** (0.030 g, 0.038 mmol) in THF-d_8 (0.7 mL) was treated with KO^{t}Bu (0.004 g, 0.039 mmol). The NMR tube was charged with 4 bar of H_2, and complete formation of **6** was confirmed by NMR spectroscopy. ^{1}H and ^{31}P{^{1}H} NMR spectroscopy analysis of the reaction mixture after 6 days did not show formation of the trihydride complex **7**.

*Evaluation of the role of **6** in the hydrogenation of **5***

In a J.Young-valved NMR tube, a suspension of complex **2** (0.010 g, 0.014 mmol) and complex **1** (0.010 g, 0.012 mmol) in THF-d_8 (0.5 mL) was pressurized with 1.5 bar of H_2 and treated with KO^{t}Bu (0.003 g, 0.027 mmol). The sample was analyzed by NMR spectroscopy after 1 h, observing the formation of complexes **5** and **6** in 1.2:1 ratio. The reaction was allowed to proceed, and followed by NMR spectroscopy at regular intervals. For example, analysis of the sample after 20 and 45 hours showed the expected signals for complex **6** and the formation of complex **4** in 46% and 82% conversion from **5**, respectively.

4. Deuteration experiment of 4

In a J.Young-valved NMR tube, a suspension of complex **4** (0.005 g, 0.007 mmol) in THF-d_8 (0.5 mL) was pressurized with 3 bar of D_2, and shaken for 20 h at room temperature. Analysis by ^{1}H NMR spectroscopy showed, in addition to deuteration of **4**, the formation of partially deuterated trihydride **7** (Figures S11-S12).

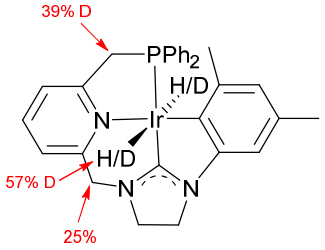

Figure S11. Degree of deuteration of **4** under 3 bar of D_2 after 20 h.

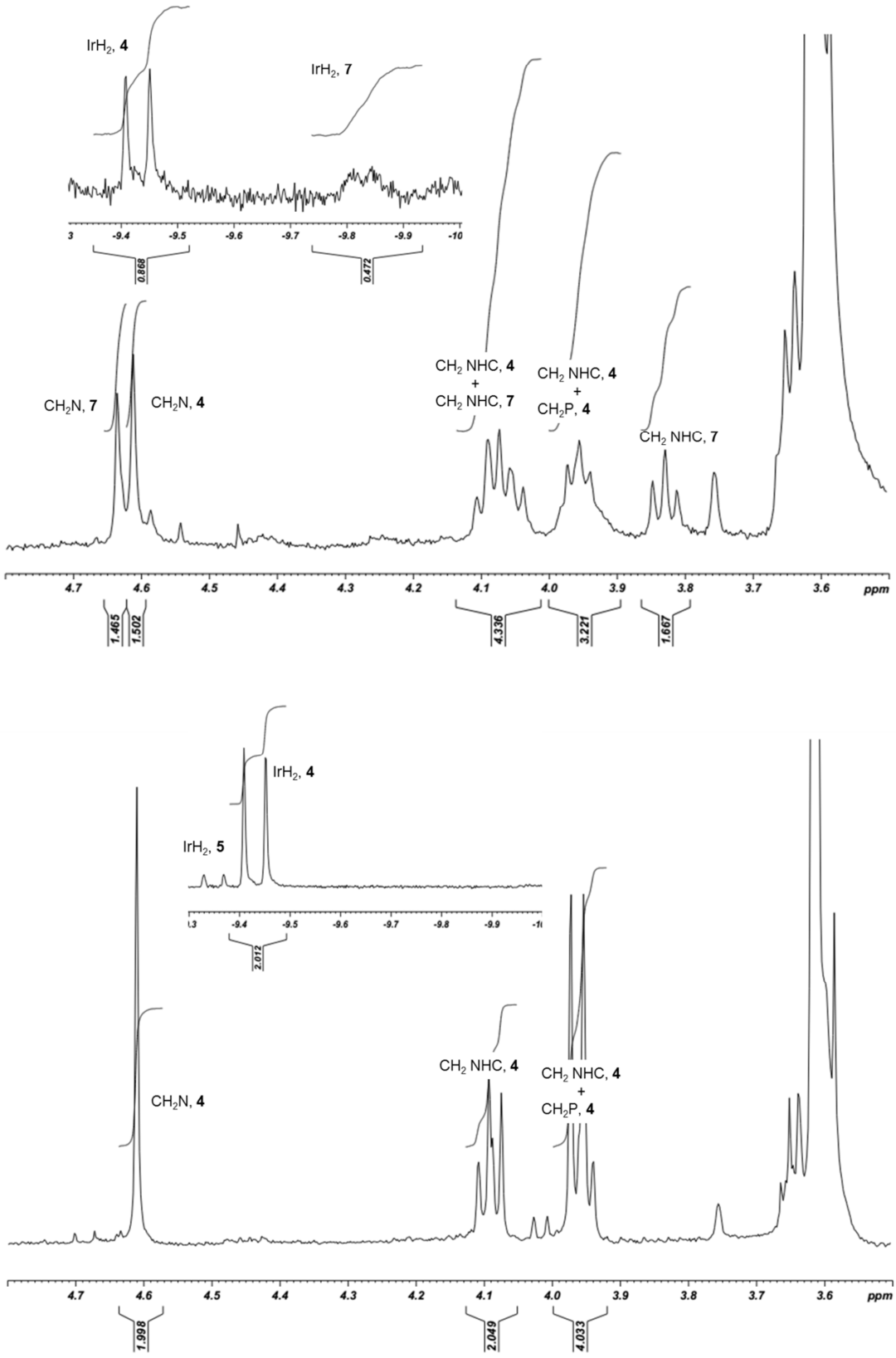

Figure S12. Selected regions of the ^{1}H NMR spectrum (500 MHz, THF-d_8) of **4** exposed to 3 bar of D_2: i) (bottom) after 20 min, ii) (top) after 20 h. Integral values referenced to the aromatic protons of the xylyl fragment.

5. Crystal X-ray structure analysis

Crystals of suitable size for X-ray diffraction analysis of **2**, **3** and **4** were coated with dry perfluoropolyether and mounted on glass fibres and fixed in a cold nitrogen stream (T = 213 K) to the goniometer head. Data collection was performed on a Bruker-Nonius X8Apex-II CCD diffractometer, using monochromatic radiation λ(Mo K_α) = 0.71073 Å, by means of ω and φ scans with a width of 0.50 degree. The data were reduced (SAINT)[2] and corrected for absorption effects by the multi-scan method (SADABS).[3] The structures were solved by direct methods (SIR-2002)[4] and refined against all F^2 data by full-matrix least-squares techniques (SHELXL-2016/6)[5] minimizing $w[F_o^2-F_c^2]^2$. All non-hydrogen atoms were refined anisotropically. The hydrogen atoms were included from calculated positions and refined riding on their respective carbon atoms with isotropic displacement parameters. A summary of cell parameters, data collection, structure solution, and refinement for these three crystal structures are given in Tables S1, S2 and S3. CCDC 1581042 (**2**), 1830214 (**3**) and 1581043 (**4**) contain the supplementary crystallographic data for this paper. These data can be obtained free of charge from The Cambridge Crystallographic Data Centre via www.ccdc.cam.ac.uk/data_request/cif.

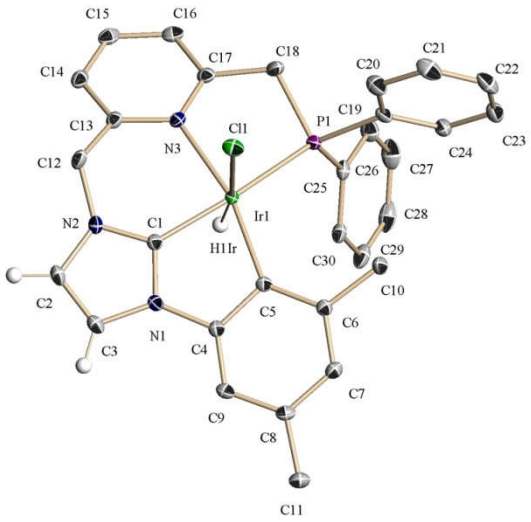

Figure S13. ORTEP view of molecular structure of complex **2** with thermal ellipsoids drawn at the 30% level. Hydrogen atoms, except the hydrido ligands and the NHC hydrogens, have been omitted for clarity.

Table S1. Crystal data and structure refinement for **2**

Empirical formula	$C_{30}H_{28}ClIrN_3P$	
Formula weight	689.17	
Temperature	193(2) K	
Wavelength	0.71073 Å	
Crystal system	Monoclinic	
Space group	$P2_1/c$	
Unit cell dimensions	a = 10.1852(2) Å	α = 90°.
	b = 17.4738(3) Å	β = 95.5380(10)°.
	c = 14.3619(3) Å	γ = 90°.
Volume	2544.12(9) $Å^3$	
Z	4	
Density (calculated)	1.799 Mg/m^3	
Absorption coefficient	5.441 mm^{-1}	
F(000)	1352	
Crystal size	0.340 x 0.280 x 0.160 mm^3	
Theta range for data collection	2.323 to 25.247°.	
Index ranges	-12<=h<=12, -10<=k<=20, -17<=l<=8	
Reflections collected	26749	
Independent reflections	4601 [R(int) = 0.0146]	
Completeness to theta = 25.242°	99.9 %	
Absorption correction	Semi-empirical from equivalents	
Max. and min. transmission	0.7461 and 0.5619	
Refinement method	Full-matrix least-squares on F^2	
Data / restraints / parameters	4601 / 1 / 330	
Goodness-of-fit on F^2	1.133	
Final R indices [I>2sigma(I)]	R1 = 0.0151, wR2 = 0.0382	
R indices (all data)	R1 = 0.0159, wR2 = 0.0386	
Extinction coefficient	n/a	
Largest diff. peak and hole	0.677 and -0.629 $e.Å^{-3}$	

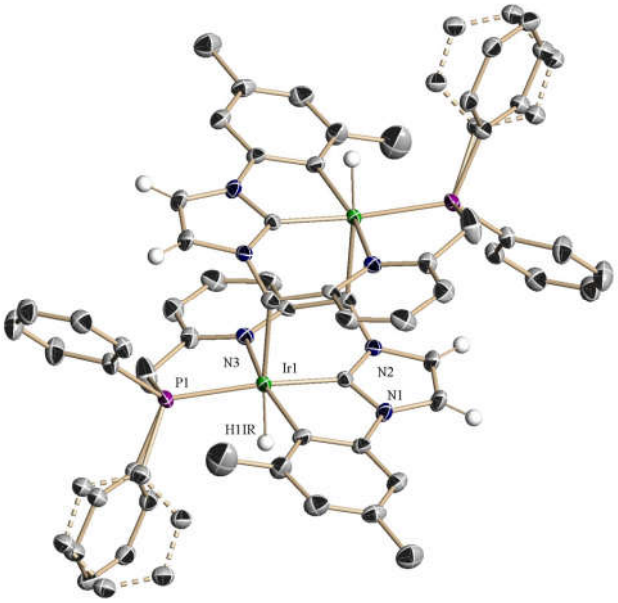

Figure S14. ORTEP view of molecular structure of dimer complex **3** with thermal ellipsoids drawn at the 30% level. Hydrogen atoms, except the hydrido ligands and the NHC hydrogens, have been omitted for clarity.

Table S2. Crystal data and structure refinement for **3**

Empirical formula	$C_{30}H_{27}IrN_3P$	
Formula weight	652.71	
Temperature	193(2) K	
Wavelength	0.71073 Å	
Crystal system	Monoclinic	
Space group	$P2_1/n$	
Unit cell dimensions	a = 12.4319(6) Å	α = 90°.
	b = 14.5003(6) Å	β = 111.232(2)°.
	c = 14.6477(6) Å	γ = 90°.
Volume	2461.25(19) $Å^3$	
Z	4	
Density (calculated)	1.761 Mg/m^3	
Absorption coefficient	5.514 mm^{-1}	
F(000)	1280	
Crystal size	0.150 x 0.100 x 0.070 mm^3	
Theta range for data collection	2.250 to 25.248°.	
Index ranges	-14<=h<=10, -17<=k<=17, -15<=l<=17	
Reflections collected	19107	
Independent reflections	4439 [R(int) = 0.0282]	
Completeness to theta = 25.242°	99.6 %	
Absorption correction	Semi-empirical from equivalents	
Max. and min. transmission	0.7461 and 0.6499	
Refinement method	Full-matrix least-squares on F^2	
Data / restraints / parameters	4439 / 337 / 352	
Goodness-of-fit on F^2	1.052	
Final R indices [I>2sigma(I)]	R1 = 0.0218, wR2 = 0.0510	
R indices (all data)	R1 = 0.0274, wR2 = 0.0533	
Extinction coefficient	n/a	
Largest diff. peak and hole	0.965 and -0.621 $e.Å^{-3}$	

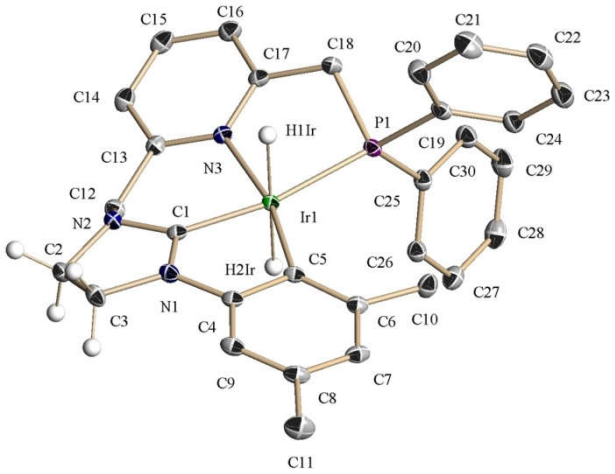

Figure S15. ORTEP view of molecular structure of complex **4** with thermal ellipsoids drawn at the 30% level. Hydrogen atoms, except the hydrido ligands and the NHC hydrogens, have been omitted for clarity.

Table S3. Crystal data and structure refinement for **4**

Empirical formula	$C_{30}H_{31}IrN_3P$	
Formula weight	656.75	
Temperature	193(2) K	
Wavelength	0.71073 Å	
Crystal system	Monoclinic	
Space group	$P2_1/n$	
Unit cell dimensions	a = 9.6983(4) Å	α = 90°.
	b = 20.8545(7) Å	β = 97.5510(10)°.
	c = 12.7013(4) Å	γ = 90°.
Volume	2546.60(16) $Å^3$	
Z	4	
Density (calculated)	1.713 Mg/m^3	
Absorption coefficient	5.330 mm^{-1}	
F(000)	1296	
Crystal size	0.200 x 0.150 x 0.100 mm^3	
Theta range for data collection	2.491 to 25.250°.	
Index ranges	-11<=h<=9, -25<=k<=25, -15<=l<=15	
Reflections collected	40654	
Independent reflections	4607 [R(int) = 0.0247]	
Completeness to theta = 25.242°	99.9 %	
Absorption correction	Multi_scan	
Max. and min. transmission	0.7461 and 0.5257	
Refinement method	Full-matrix least-squares on F^2	
Data / restraints / parameters	4607 / 2 / 326	
Goodness-of-fit on F^2	1.058	
Final R indices [I>2sigma(I)]	R1 = 0.0155, wR2 = 0.0386	
R indices (all data)	R1 = 0.0176, wR2 = 0.0393	
Extinction coefficient	n/a	
Largest diff. peak and hole	1.113 and -0.567 $e.Å^{-3}$	

6. DFT calculations

DFT calculations were carried out with the Gaussian 09 program.[6] The PBE0 functional[7] was used, with dispersion effects taken into account by adding the D3 version of Grimme's empirical dispersion.[8] C, H, N and P atoms were represented by the 6-31g(d,p) basis set,[9] whereas Ir was described using the Stuttgart/Dresden Effective Core Potential and its associated basis set SDD.[10] All geometry optimizations were performed in the gas phase without restrictions. Vibrational analysis was used to characterize the stationary points in the potential energy surface, as well as for calculating the Zero-point, Enthalpy and Gibbs energy corrections at 295 K and 1 atm. The nature of the intermediates connected by a given transition state along a reaction path was proven by IRC calculations or by perturbing the geometry of the TS along the reaction path eigenvector and optimizing to the corresponding minima. Bulk solvent effects (THF) were modelled with the SMD continuum model.[11]

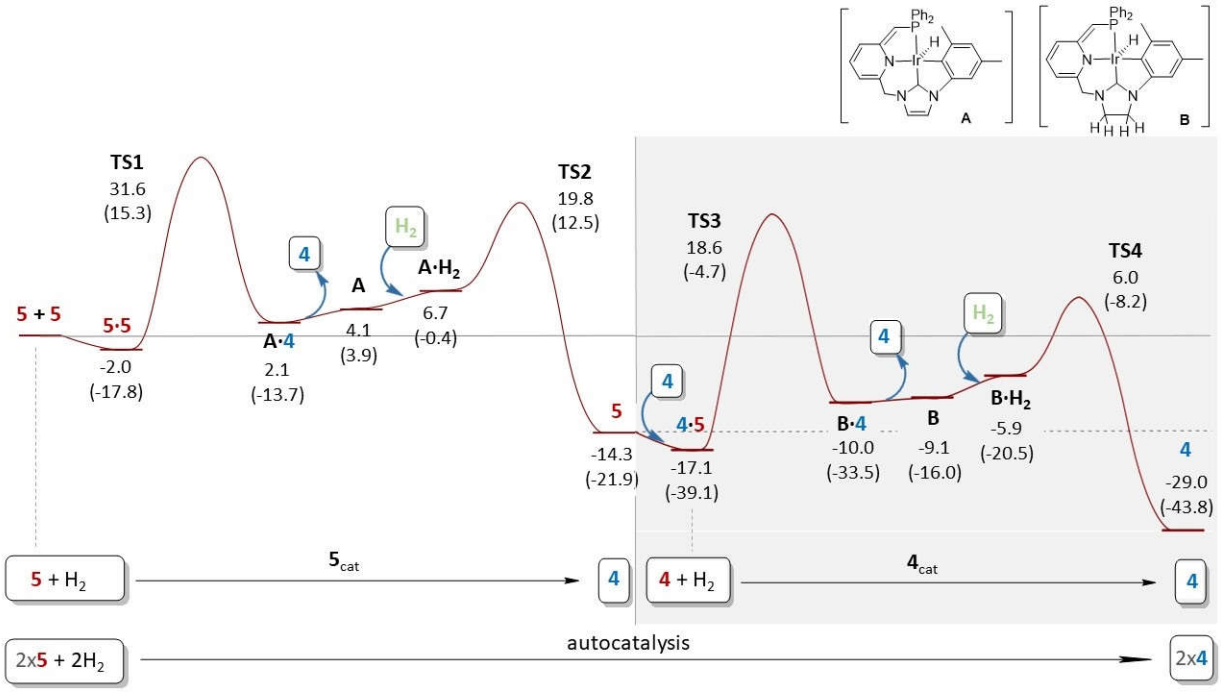

Figure S16. DFT calculated energy profile for self-hydrogenation of the imidazol-2-ylidene complex **5**. Data are free energy in THF (kcal·mol^{-1}) relative to 2x**5** + 2xH_2. Data in parenthesis corresponds to Δ*ZPE* in THF.

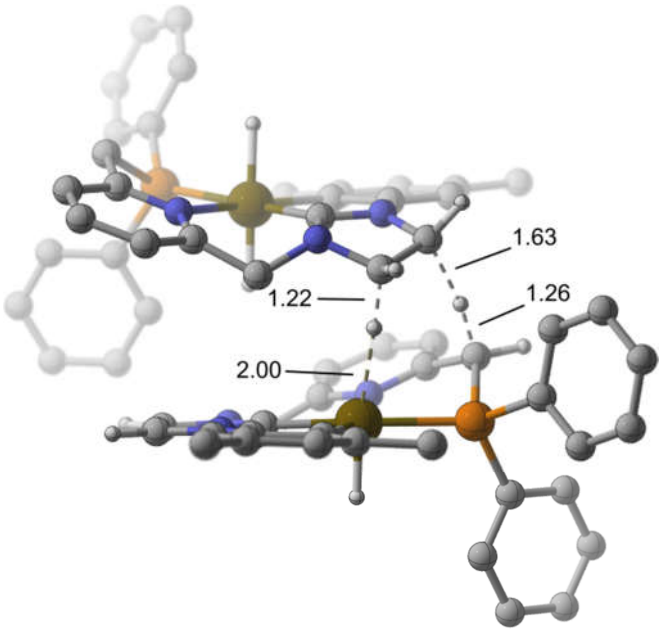

Figure S17. DFT-optimized geometries of **TS1**.

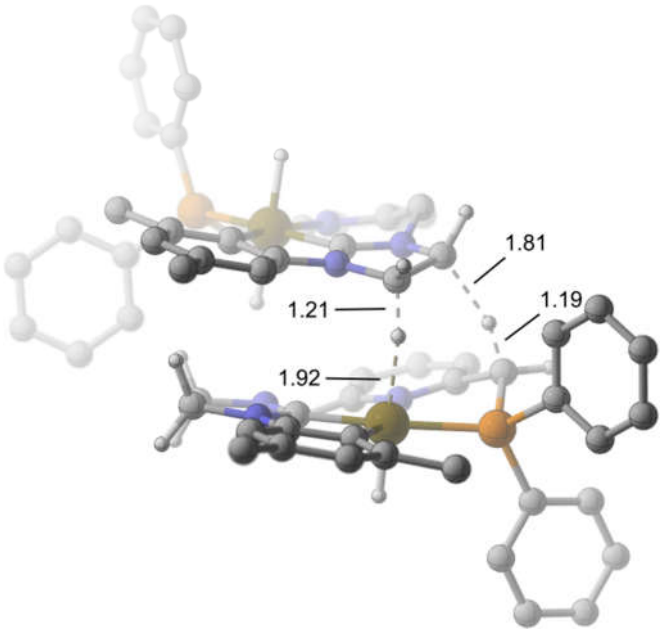

Figure S18. DFT-optimized geometries of **TS3**.

7. References

1. P. Sánchez, M. Hernández-Juárez, E. Álvarez, M. Paneque, N. Rendón and A. Suárez, *Dalton Trans.*, 2016, **45**, 16997-17009.
2. Bruker. SAINT. *APEX2* **2007**, Bruker AXS Inc., Madison, Wisconsin, USA.
3. a) G. M. Sheldrick, SADABS, Programs for Scaling and Absorption Correction of Area Detector Data. *SADABS, Programs Scaling Absorpt. Correct. Area Detect. Data* **1997**, University of Göttingen: Göttingen, Germany; b) Bruker. SADABS. *APEX2* **2007**, Bruker AXS Inc., Madison, Wisconsin, USA.
4. M. C. Burla, M. Camalli, B. Carrozzini, G. L. Cascarano, C. Giacovazzo, G. Polidori and R. Spagna, SIR2002 : The Program. *J. Appl. Crystallogr.*, 2003, **36** (4), 1103–1103. DOI: 10.1107/S0021889803012585.
5. a) G. M. Sheldrick, A Short History of SHELX. *Acta Crystallographica Section A: Foundations of Crystallography*. 2008, pp 112–122. DOI: 10.1107/S0108767307043930; b) G. M. Sheldrick, *Acta Cryst.*, 2015, **C71**, 3-8. DOI: 10.1107/S2053229614024218.
6. Gaussian 09, Revisions B.01 and E.01, M. J. Frisch, G. W. Trucks, H. B. Schlegel, G. E. Scuseria, M. A. Robb, J. R. Cheeseman, G. Scalmani, V. Barone, G. A. Petersson, H. Nakatsuji, X. Li, M. Caricato, A. Marenich, J. Bloino, B. G. Janesko, R. Gomperts, B. Mennucci, H. P. Hratchian, J. V. Ortiz, A. F. Izmaylov, J. L. Sonnenberg, D. Williams-Young, F. Ding, F. Lipparini, F. Egidi, J. Goings, B. Peng, A. Petrone, T. Henderson, D. Ranasinghe, V. G. Zakrzewski, J. Gao, N. Rega, G. Zheng, W. Liang, M. Hada, M. Ehara, K. Toyota, R. Fukuda, J. Hasegawa, M. Ishida, T. Nakajima, Y. Honda, O. Kitao, H. Nakai, T. Vreven, K. Throssell, J. A. Montgomery, Jr., J. E. Peralta, F. Ogliaro, M. Bearpark, J. J. Heyd, E. Brothers, K. N. Kudin, V. N. Staroverov, T. Keith, R. Kobayashi, J. Normand, K. Raghavachari, A. Rendell, J. C. Burant, S. S. Iyengar, J. Tomasi, M. Cossi, J. M. Millam, M. Klene, C. Adamo, R. Cammi, J. W. Ochterski, R. L. Martin, K. Morokuma, O. Farkas, J. B. Foresman and D. J. Fox, Gaussian, Inc., Wallingford CT, 2016.
7. S. Grimme, J. Antony, S. Ehrlich and H. Krieg, *J. Chem. Phys.*, 2010, **132**, 154104.
8. a) C. Adamo, V. Barone. *J. Chem. Phys.* **1999**, *110*, 6158-6169; b) This functional has been shown to reproduce the uniform electron gas limit (UEG) and being effective in describing metal hydride, dihydrogen and hydrogen bond situations; D. A. Pantazis, J. E. McGrady, F. Maseras and M. Etienne, *J. Chem. Theor. Comput.*, 2007, **3**, 1329-1336.
9. a) W. J. Hehre, R. Ditchfield and J. A. Pople, *J.* Phys. *Chem.*. 1972, **56**, 2257-2261; b) P. C. Hariharan and J. A. Pople, *Theor. Chim. Acta.*, 1973, **28**, 213-222; c) M. M. Francl, W. J. Pietro, W. J. Hehre, J. S. Binkley, M. S. Gordon, D. J. DeFrees and J. A. Pople, *Chem. Phys.*, 1982, **77**, 3654-3665.
10. D. Andrae, U. Haeussermann, M. Dolg, H. Stoll and H. Preuss, *Theor. Chim. Acc.*, 1990, **77**, 123-141.
11. A. V. Marenich, C. J. Cramer and D. G. Truhlar, *J. Phys. Chem. B*, 2009, **113**, 6378-6396.